International Journal of Electrical, Electronic and Communication Sciences
ISSN: 2517-9438
Vol:12, No:10, 2018

Noise Performance of Magnetic Field Tunable Avalanche Transit Time Source

Partha Banerjee, Aritra Acharyya, Arindam Biswas, A. K. Bhattacharjee, Amit Banerjee, Hiroshi Inokawa

***Abstract*—**The effect of magnetic field on the noise performance of the magnetic field tunable avalanche transit time (MAGTATT) device based on Si, designed to operate at W-band (75 – 110 GHz), has been studied in this paper. A comprehensive two-dimensional (2D) model has been developed. The simulation results show that due to the presence of applied external transverse magnetic field, both the noise spectral density and noise measure of the MAGTATT device increase significantly. The noise performance of the device has been found to be further deteriorated if the magnetic field strength is further increased. Hence, in order to achieve the magnetic field tuning of the radio frequency (RF) properties of impact avalanche transit time (IMPATT) source, the noise performance of it has to be sacrificed in fair extent. Moreover, it clearly indicates that an IMPATT source must be covered with appropriate magnetic shielding material to avoid undesirable shift in operating frequency and output power and objectionable amount of deterioration in noise performance due to the presence of external magnetic field.

***Keywords*—**2-D model, IMPATT, MAGTATT, mm-wave, noise performance.

I. Introduction

IMPATT diodes are special diode structures which exhibit negative resistance under suitable reverse biased condition. IMPATT diodes are used as oscillators to generate significantly high power at microwave and millimeter-wave frequencies (1-300 GHz) [32]. However, the advantage of high power applications comes on trade-off with a major drawback, i.e. significantly high level of noise, generated from the statistical nature of the avalanche process within reverse biased IMPATT device. The bias current tuning of IMPATT oscillators enables the modulation of RF power as well as operating frequency of the source. Thus the bias current is the firsthand manual tuning parameter for power and frequency tuning of IMPATT sources, known as electronic tuning [1]. On the other hand, the optical tuning is an additional tuning mechanism for the modulation of power and frequency of IMPATT sources [2]-[5]. Other than these tuning methods, another method is also available for the external control of the IMPATT properties, which is the magnetic field tuning. The application of magnetic field in reverse biased IMPATT diode causes a number of effects in its microelectronic operation: (a) changes of the carrier motion, (b) carrier redistribution and (c) redistribution of electrostatic potential. The effect of magnetic field on the device properties can be imagined in terms of Hall voltage or carrier deflection. Glance et al. first reported the experimental magnetic field tuning of the operating frequency of IMPATT oscillators [6]. They carried out the said experiment on the measured frequency and output power of an X-band (8-12 GHz) ferrite-filled microstrip resonator based IMPATT oscillator. They investigated the influence of static magnetic field along the direction of RF propagation and along the direction of the RF magnetic field [6]. Around 17 MHz Oe^{-1} (Oe ≡ Oersted), frequency change was observed when the magnetic field was applied along the direction of RF propagation. The variation of the permeability of ferrite material from the demagnetized state to the saturation state was the primary cause of the magnetic field induced frequency tuning of microstrip IMPATT oscillator [7]. Later, Hartnagel et al. experimentally demonstrated the magnetic field tuning of frequency and power output of a 7.480 GHz double-drift region (DDR) IMPATT oscillator [8]. They obtained decrease in the operating frequency of the oscillator in order of 20 to 380 KHz due to application of the static magnetic field of 0.4 to 1.6 kG (G ≡ Gauss) in perpendicular direction of the carrier transport within the device. So long, no credible model for the analysis of the above-discussed phenomena was established; but in 2016, Banerjee et al. have developed a complete 2-D large-signal model to study the effect of transverse magnetic field on the DC and large-signal properties of IMPATT diodes [9]. The sensitivity of various static and large-signal parameters on externally applied transverse steady magnetic field of a DDR IMPATT diode, designed to operate at 94 GHz, have been studied. The structure and arrangement proposed by them may be considered as MAGTATT device.

The MAGTATT device has immense potential to be used in various areas of communication systems such as phased array antennas for space based communication, active phased array Radar systems, etc. However, IMPATTs/MAGTATTs are noisy devices and the primary source of noise in these is the random nature of the impact ionizing phenomena [10]-[16]. Hence the complete high frequency behavior of IMPATT/ MAGTATT device remains incomplete if the noise performance of the device under practical operating conditions

P. Banerjee is with the Department of Electronics and Communication Engineering, Academy of Technology, West Bengal University of Technology, Adisaptagram, Hooghly, West Bengal 712121, India (e-mail: partha_ban@yahoo.com).

A. Acharyya is with the Department of Electronics and Communication Engineering, Cooch Behar Government Engineering College, Harinchawra, Ghughumari, West Bengal 736170, India (e-mail: ari_besu@yahoo.co.in).

A. Biswas is with the Department of Electronics and Communication Engineering, Asansol Engineering College, Vivekananda Sarani, Kanyapur, Asansol, West Bengal 713305, India (e-mail: mailarindambiswas@yahoo.co.in).

A. K. Bhattacharjee is with the Department of Electronics and Communication Engineering, National Institute of Technology, Durgapur, West Bengal 713209, India (e-mail: akb_bet@gmail.com).

A. Banerjee, and H. Inokawa are with the Research Institute of Electronics, Shizuoka University, 3-5-1 Johoku, Naka-ku, Hamamatsu 432-8011, Japan (e-mail: amit_ban@refiffmail.com, inokawa.h@gmail.com).

has not been studied. In this work, a comprehensive 2-D model for studying the avalanche noise behavior of the MAGTATT device has been developed by the authors. Simulations have been carried out to study the noise performance of MAGTATT device based on Si, designed to operate at W-band by calculating the noise spectral density and noise measure of the device as functions of frequency in absence as well as in presence of the transverse magnetic field. The 2-D simulation technique presented in this paper has also been validated by comparing the simulation results with the numerical results reported earlier [16], [17].

II. Three-Dimensional Model

In order to simplify the three-dimensional (3D) modeling of the device, the cross-sectional shape of the MAGTATT device is assumed to be rectangular instead of circular [9], [18]. This also simplifies the mathematical modeling of the arrangement of transverse magnetic field coupling with the reverse biased MAGTATT structure. This further ensures the use of Cartesian coordinate system which is more convenient than the cylindrical coordinate system. However, the shape of the cross-section of the diode does not affect the simulation results, since only the cross-sectional area of the diode is utilized in calculations, not the shape of the cross-section. The 3-D model of the device structure under investigation is shown in Fig. 1. However, in the current modeling, it is found that the consideration of z-direction is unnecessary, and 2-D model is enough for the analysis, the reason behind this is discussed in details later. In the present model, the cross-sectional shape of the metallurgical junction (i.e. the n-p junction) is taken to be rectangular for simplicity as mentioned earlier [19]. The lengths of n^+, n, p, p^+-layers are denoted by W_{n+}, W_n, W_p and W_{p+} respectively in Fig. 1. The doping concentrations of the above mentioned layers are denoted by N_{n+}, N_D, N_A and N_{p+} respectively. Width of the device along x-direction is D and height of the device along z-direction is H. Thus the cross-sectional area of the metallurgical junction is $A_j = DH$.

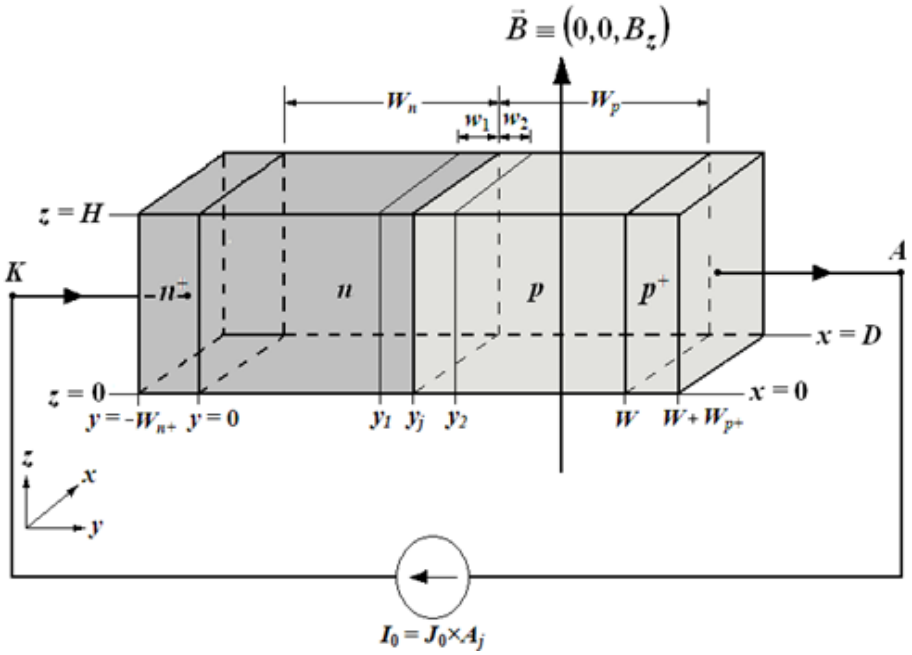

Fig. 1 3D model of the n^+-n-p-p^+ structured DDR IMPATT diode ($w_1 = w_2 = 0.1$ μm) [9]

TABLE I
Structural and Doping Parameters [9]

Design parameters	Values
W_n (μm)	0.400
W_p (μm)	0.380
N_D ($\times 10^{23}$ m^{-3})	1.200
N_A ($\times 10^{23}$ m^{-3})	1.250
N_{n+} ($\times 10^{25}$ m^{-3})	5.000
N_{p+} ($\times 10^{25}$ m^{-3})	2.700
A_j (m^{-2})	9.6211×10^{-10}

The MAGTATT device based on Si has been already designed to operate at W-band (75 – 110 GHz) in the earlier work by the authors by choosing the optimum values of W_n, W_p, N_D, N_A, N_{n+} and N_{p+} [9], [18], [20]. The structural as well as doping parameters of the device are given in Table I. The width (along x-direction) and height (along z-direction) of the diode have been taken as D = 10.0 μm and H = 96.211 μm respectively. Therefore the junction area of the diode is $A_j = DH = 9.6211 \times 10^{-10}$ m^2 which is the same as the junction area of the diode having circular cross-section of radius of 35.0 μm [21].

III. 2-D Model for DC Simulation

The carrier transport within the device occurs along y-

direction in the absence of magnetic field. In presence of the magnetic field along +*z*-direction, the Lorentz force deflects the charge carriers into the Hall direction, i.e. either +*x*-direction or –*x*-direction depending on the polarity of the charge carriers. If the magnetic field is applied perpendicular to the *xy*-plane, i.e. if the magnetic field has only the *z*-component (magnetic flux density $\vec{B} \equiv (0,0,B_z)$), then the deflection of the charge carriers which are flowing along ±*y*-direction, are bound to occur along ±*x*-direction as per the direction of the $\vec{B}$ (i.e. along either +*z*-direction or –*z*-direction). Thus, the distributions of charge carriers are functions of only the space coordinates *x* and *y*. Therefore the problem can easily be reduced to a 2D problem depending only on *x* and *y*-coordinates. Due to the Lorentz force in presence of the magnetic field, the fundamental device equations in steady-state can be written as [9], [22]

(a) Poisson's Equation:

$$\vec{\nabla}^2 V^{(\vec{B})}(x,y) = -\frac{q}{\varepsilon_s}\left(p^{(\vec{B})}(x,y) - n^{(\vec{B})}(x,y) + N(x,y)\right), \quad (1)$$

(b) Steady-State Continuity Equations:

$$\left(\frac{1}{q}\right)\vec{\nabla}\cdot\vec{J}_{p,n}^{(\vec{B})}(x,y) = \pm\begin{pmatrix} G_{A_p,A_n}^{(\vec{B})}(x,y) + G_{T_p,T_n}^{(\vec{B})}(x,y) \\ -R_{p,n}^{(\vec{B})}(x,y) \end{pmatrix}, \quad (2)$$

(c) Current Density Equations:

$$\vec{J}_{p,n}^{(\vec{B})}(x,y) = \left(\frac{1}{1+\left(\mu_{p,n}^{*}\vec{B}\right)^2}\right)\begin{bmatrix} \begin{pmatrix} q\mu_{p,n}\left(p^{(\vec{B})},n^{(\vec{B})}(x,y)\right)\vec{\xi}^{(\vec{B})}(x,y) \\ \mp qD_{p,n}\vec{\nabla}\left(p^{(\vec{B})},n^{(\vec{B})}(x,y)\right) \end{pmatrix} \\ -\mu_{p,n}^{*}\vec{B}\times\begin{pmatrix} q\mu_{p,n}\left(p^{(\vec{B})},n^{(\vec{B})}(x,y)\right)\vec{\xi}^{(\vec{B})}(x,y) \\ \mp qD_{p,n}\vec{\nabla}\left(p^{(\vec{B})},n^{(\vec{B})}(x,y)\right) \end{pmatrix} \end{bmatrix} \quad (3)$$

where $V^{(\vec{B})}(x,y)$ is the electric potential (electric field $\vec{\xi}^{(\vec{B})}(x,y) = -\vec{\nabla}V^{(\vec{B})}(x,y)$), $\vec{J}_p^{(\vec{B})}(x,y)$ and $\vec{J}_n^{(\vec{B})}(x,y)$ denote electron and hole current densities, $p^{(\vec{B})}(x,y)$ and $n^{(\vec{B})}(x,y)$ denote electron and hole concentrations at the space point (*x*,*y*) under the magnetic field of $\vec{B}$ and ε_s is the permittivity of the semiconductor. Moreover, μ_n and μ_p are the drift mobilities, μ_n^* and μ_p^* are the Hall mobilities, D_n and D_p are the diffusion constants of electrons and holes respectively, q is the elementary charge ($q = 1.6\times10^{-19}$ C), $\vec{\nabla} \equiv (\partial/\partial x)\hat{x} + (\partial/\partial y)\hat{y}$ is the 2-D del operator; where $\hat{x}$ and $\hat{y}$ are the unit vectors along *x* and *y*-directions respectively. Two important electron-hole pair (EHP) generation mechanisms such as avalanche ($G_{A_p,A_n}^{(\vec{B})}(x,y)$) and band-to-band tunneling ($G_{T_p,T_n}^{(\vec{B})}(x,y)$) generations are taken into account in the present model. Detailed expressions of the avalanche and band-to-band tunneling generation rate of charge carriers as functions of electric field under perpendicular magnetic field as well as the recombination rate ($R_{p,n}(x,y)$) of those within the depletion layer of the device have already been reported by the authors [9]. Due to the limitation in space, the above mentioned expressions are not repeated in the present paper. The molecular beam epitaxy (MBE) growth technique is the most favorable process to fabricate MAGTATT device designed to operate at W-band [9], [21]. However, for the mathematical formulation of the 2D doping profile ($N(x,y)$) of the device a simple formulation of diffusion growth technique has been adopted. By optimizing some important parameters related to the diffusion technique, sharp and most favorable doping profile of the device has been selected which nearly matches with the MBE grown structure [9], [19], [21], especially for the devices operating at or above 94 GHz. The 2D doping profile of the device has been formulated as [9], [23]

$$\left.\begin{aligned} N(x,y) &= N_{n^+}\exp\left(-1.08\lambda_n(y) - 0.78\lambda_n(y)^2\right) && y \le 0 \\ &= N_D && 0 < y \le y_1 \\ &= N_D\left[1 - \exp\left(\frac{y}{s}\right)\right] && y_1 < y \le y_j \\ &= -N_A\left[\exp\left(-\frac{y}{s}\right) - 1\right] && y_j < y \le y_2 \\ &= -N_A && y_2 < y < W \\ &= -N_{p^+}\exp\left(-1.08\lambda_p(y) - 0.78\lambda_p(y)^2\right) && y \ge W \end{aligned}\right\} 0 \le x \le D \quad , (4)$$

where $\lambda_n(y) = \left(W_{n^+} + y\right)\big/2\sqrt{Dt_d}$ and $\lambda_p(y) = \left(W_{p^+} + y - W\right)\big/2\sqrt{Dt_d}$, D is the impurity diffusion constant, t_d is the time for diffusion, *s* is a constant whose value may be taken as ≈ 5 nm and W is the depletion layer width ($W = W_n + W_p$). The value of the Dt_d is taken to be $Dt_d \approx 4.0\times10^{-12}$ m^{-2}. Here the doping profile near the *n*-*p* junction (within $y_1 < y \le y_2$) has been approximated by incorporating an appropriate exponential function, while the doping profiles near the *n*-n^+ and *p*-p^+ interfaces (i.e. $y \le 0$ and $y \ge W$ respectively) are taken into account by an equivalent complementary error function [24]. The values of the parameters *s* and Dt_d are optimized to obtain the most favorable doping profiles of the device which nearly match with the MBE grown n^+-*n*-*p*-p^+ MAGTATT structure for operation at 94 GHz and above. The n^+-*n* and p^+-*p* interfaces at $y = 0$ and $y = W$ respectively are effectively considered as ohmic contacts; since the doping concentrations of n^+- and p^+-layers are almost 10^3 times higher as compared to those of *n*- and *p*-epitaxial layers. Thus the boundary conditions for the electric potentials at $y = 0$ and $y = W$ for $0 \le x \le D$ are given by

$$\left.\frac{\partial V^{(\vec{B})}(x,y)}{\partial y}\right|_{y=0,W} = 0 \qquad 0 \le x \le D. \quad (5)$$

The boundary conditions associated with electron and hole components of current densities have been imposed at $y = 0$ and $y = W$ for $0 \le x \le D$ via

$$\vec{P}^{(\vec{B})}(x,(y=0,W))=\left[\mp 1\pm\frac{2\vec{J}_{p,n}^{(\vec{B})}(x,(y=0,W))}{\vec{J}_{p}^{(\vec{B})}(x,(y=0,W))+\vec{J}_{n}^{(\vec{B})}(x,(y=0,W))}\right] \quad 0\le x\le D, \qquad (6)$$

where the normalized current density parameter ($\vec{P}(x,y)$) may be defined as

$$\vec{P}^{(\vec{B})}=\left(\frac{\vec{J}_{p}^{(\vec{B})}(x,y)-\vec{J}_{n}^{(\vec{B})}(x,y)}{\vec{J}_{p}^{(\vec{B})}(x,y)+\vec{J}_{n}^{(\vec{B})}(x,y)}\right). \qquad (7)$$

Along the floating boundaries, i.e. at $x = 0$ and $x = D$ for $0 \le y \le W$, the current density boundary conditions can be written as

$$\vec{J}_{p,n}^{(\vec{B})}((x=0,D),y)=0 \qquad 0\le y\le W. \qquad (8)$$

As per space charge boundary conditions along the floating boundaries, the following conditions are adopted [23]

$$\frac{\partial^2}{\partial^2 x}\left[p^{(\vec{B})}((x=0,D),y)-n^{(\vec{B})}((x=0,D),y)+N((x=0,D),y)\right]=0 \quad 0\le y\le W. \qquad (9)$$

Equation (9) is obviously less restraining than the condition of zero space charge variation proposed by Kurata [25]. The asymmetry introduced in the present problem by the applied magnetic field is the primary cause of using (9).

The set of equations (1)-(3) constitutes the complete system to be solved subject to appropriate boundary conditions given in (5)-(9). The finite difference discretizations of (1), (3), (5), (6), (8) and (9) have been set up by following the procedure adopted in earlier reports [25], [26]. However, a discretization technique similar to the generalized Scharfetter-Gummel scheme proposed by Rudan and Guerrieri has been used for the continuity equations given by (2) which include the magnetic field through (3) [27]. The simultaneous solution of the fully coupled Poisson's equation, continuity equations and current density equations have been obtained subject to the boundary conditions given in (5)-(9) by linearizing the said equations by applying Newton's iteration principle. Solution of the aforementioned system of equations provide important static or DC parameters such as electric potential ($V^{(\vec{B})}(x,y)$), electric field ($\vec{\xi}^{(\vec{B})}(x,y)$), carrier current densities ($\vec{J}_{p,n}^{(\vec{B})}(x,y)$) and carrier concentrations ($p^{(\vec{B})},n^{(\vec{B})}(x,y)$) as functions of both space coordinates x and y under applied magnetic field of $\vec{B}\equiv(0,0,B_z)$.

IV. 2D Model for Noise Simulation

The noise simulation of MAGTATT device requires the outcomes of the DC simulation as the inputs. Output of the noise simulation program provides vital noise parameters such as noise spectral density and noise measure as functions of frequency (f) [18]. The primary source of noise in avalanche transit time (ATT) devices is the random generation of EHPs caused by impact ionization. This leads to fluctuations of DC current and electric field which are equivalent to small-signal AC components of the respective parameters even in the absence of time varying voltage across the device [18]. Thus the noise analysis is concerned with the open circuit condition of the device in which time varying applied voltage is not applied. Starting from the small-signal noise fields along x- and y-directions due to the application of the magnetic field along z-direction given by

$$\left.\begin{aligned}\vec{e}_{n}^{(\vec{B})}(x,x')&=\vec{e}_{nr}^{(\vec{B})}(x,x')+i\,\vec{e}_{ni}^{(\vec{B})}(x,x')\\ \vec{e}_{n}^{(\vec{B})}(y,y')&=\vec{e}_{nr}^{(\vec{B})}(y,y')+i\,\vec{e}_{ni}^{(\vec{B})}(y,y')\end{aligned}\right\}, \qquad (10)$$

respectively (where $i = \sqrt{-1}$), four second order differential equations in the real ($\vec{e}_{nr}^{(\vec{B})}(x,x'),\vec{e}_{nr}^{(\vec{B})}(y,y')$) and imaginary ($\vec{e}_{ni}^{(\vec{B})}(x,x'),\vec{e}_{ni}^{(\vec{B})}(y,y')$) parts of the noise fields $\vec{e}_{n}^{(\vec{B})}(x,x')$ and $\vec{e}_{n}^{(\vec{B})}(y,y')$ are framed [14], [16]-[19]. These second order differential equations are given by

$$\begin{aligned}&\frac{\partial^2\vec{e}_{nr,ni}^{(\vec{B})}(x,x')}{\partial x^2}+\left(\alpha_{n(SC)}(x)-\alpha_{p(SC)}(x)\right)\frac{\partial\vec{e}_{nr,ni}^{(\vec{B})}(x,x')}{\partial x}\\&-\left(\frac{2r_n(x)\omega}{\bar{v}(x)}\right)\frac{\partial\vec{e}_{ni,nr}^{(\vec{B})}(x,x')}{\partial x}\\&+\left[\left(\frac{\omega^2}{\bar{v}(x)^2}\right)-H(x)-\left(\frac{qr_p(x)}{\bar{v}(x)\varepsilon_s}\right)\left(\frac{\partial\left(G_{Tn}(x)+G_{Tp}(x)\right)}{\partial\xi(x)}\right)\right]\vec{e}_{nr,ni}^{(\vec{B})}(x,x')\\&-\left(\frac{2\bar{\alpha}(x)\omega}{\bar{v}(x)}\right)\vec{e}_{ni,nr}^{(\vec{B})}(x,x')=\left\{\left(\frac{2qr_p(x)\gamma(x')}{\bar{v}(x)\varepsilon_s}\right),0\right\}\end{aligned} \qquad (11)$$

$$\begin{aligned}&\frac{\partial^2\vec{e}_{nr,ni}^{(\vec{B})}(y,y')}{\partial y^2}+\left(\alpha_{n(SC)}(y)-\alpha_{p(SC)}(y)\right)\frac{\partial\vec{e}_{nr,ni}^{(\vec{B})}(y,y')}{\partial y}\\&-\left(\frac{2r_n(y)\omega}{\bar{v}(y)}\right)\frac{\partial\vec{e}_{ni,nr}^{(\vec{B})}(y,y')}{\partial y}\\&+\left[\left(\frac{\omega^2}{\bar{v}(y)^2}\right)-H(y)-\left(\frac{qr_p(y)}{\bar{v}(y)\varepsilon_s}\right)\left(\frac{\partial\left(G_{Tn}(y)+G_{Tp}(y)\right)}{\partial\xi(y)}\right)\right]\vec{e}_{nr,ni}^{(\vec{B})}(y,y')\\&-\left(\frac{2\bar{\alpha}(y)\omega}{\bar{v}(y)}\right)\vec{e}_{ni,nr}^{(\vec{B})}(y,y')=\left\{\left(\frac{2qr_p(y)\gamma(y')}{\bar{v}(y)\varepsilon_s}\right),0\right\}\end{aligned} \qquad (12)$$

where

$$\begin{aligned}&\bar{v}(x)=\left(v_n(x)v_p(x)\right)^{\frac{1}{2}},\ \bar{v}(y)=\left(v_n(y)v_p(y)\right)^{\frac{1}{2}},\\&\bar{\alpha}(x)=\left(\alpha_n(x)v_n(x)+\alpha_p(x)v_p(x)\right)/2\bar{v}(x),\\&\bar{\alpha}(y)=\left(\alpha_n(y)v_n(y)+\alpha_p(y)v_p(y)\right)/2\bar{v}(y),\\&r_{p,n}(x)=\left(v_n(x)\pm v_p(x)\right)/2\bar{v}(x),\end{aligned}$$

$$r_{p,n}(y)=\left(v_n(y)\pm v_p(y)\right)/2\bar{v}(y),$$
$$H(x)=\left(2J_0/\bar{v}(x)\varepsilon_s\right)\left(\partial\bar{\alpha}(x)/\partial\xi(x)\right)+\left(\partial(\alpha_p(x)-\alpha_n(x))/\partial\xi(x)\right)\left(\partial\xi_s(x)/\partial x\right),$$
$$H(y)=\left(2J_0/\bar{v}(y)\varepsilon_s\right)\left(\partial\bar{\alpha}(y)/\partial\xi(y)\right)+\left(\partial(\alpha_p(y)-\alpha_n(y))/\partial\xi(y)\right)\left(\partial\xi_s(y)/\partial y\right),$$
$$\xi_s(x)=\xi(x)-(q/\varepsilon_s)\int_{x=0}^{x=D}N(x)dx,$$
$$\xi_s(y)=\xi(y)-(q/\varepsilon_s)\int_{y=0}^{y=W}N(y)dx \text{ and } \omega=2\pi f.$$

The space dependent material parameters such as ionization rate ($\alpha_{p,n}(x,y)$) and drift velocity ($v_{p,n}(x,y)$) of charge carriers are functions of electric field [18]. Since the solution of the steady-state fundamental device equation (1)-(3) provides the DC electric field distribution ($\vec{\xi}(x,y)$ vs. x vs. y) within the space charge region of the device, all the afore mentioned field dependent parameters are nothing but the outcomes of the DC simulation which are included in (11) and (12) in order to obtain the noise parameters of the device in absence of in presence of the magnetic field.

The noise fields are assumed to be due to noise sources $\gamma(x')=\alpha_n(x')v_n(x')n(x')+\alpha_p(x')v_p(x')p(x')$ and $\gamma(y')=\alpha_n(y')v_n(y')n(y')+\alpha_p(y')v_p(y')p(y')$ located at the space point x' and y' respectively within the space charge region of the device [16]-[19]. Simultaneous numerical solutions of (11) and (12) subject to appropriate boundary conditions at the depletion layer edges are obtained by using Runge-Kutta method [16]-[19]. The boundary conditions at the floating boundaries, i.e. at $x = 0$ and $x = D$ for $0 \le y \le W$ are given by

$$\left[\mp\frac{i\omega}{v_{n,p}(x)}+\frac{\partial}{\partial x}\right]\vec{e}_n^{(\vec{B})}(x,x')=0 \text{ at } (x=0,D), \text{ for } 0\le y\le W. \tag{13}$$

Similarly the boundary conditions at n^+-n and p^+-p interfaces, i.e. at $x = 0$ and $x = W$ for $0 \le x \le D$ are given by

$$\left[\mp\frac{i\omega}{v_{n,p}(y)}+\frac{\partial}{\partial y}\right]\vec{e}_n^{(\vec{B})}(y,y')=0 \text{ at } (y=0,W), \text{ for } 0\le x\le D. \tag{14}$$

The procedure described in earlier reports is followed to obtain the distribution of noise field in the depletion layer of the device from simultaneous solution of (11) and (12) subject to boundary conditions given in (13) and (14) respectively [16]-[19]. In order to calculate the noise field along x-direction, the noise source $\gamma(x')$ is first taken at one end of the device, i.e. at $x = 0$ (for all $y\in[0,W]$). Then $\gamma(x')$ is shifted to the next space point and the procedure is repeated until the other end of the device ($x = D$, $y\in[0,W]$) is reached. Similarly, noise field along y-direction has been calculated by shifting the noise source $\gamma(y')$ from $y = 0$ to $y = W$ for all $x\in[0,D]$. Now the magnitude of the resultant noise field under perpendicular magnetic field can be obtained as

$$\left|\vec{e}_n^{(\vec{B})}\left((x,x'),(y,y')\right)\right|=\left(\left|\vec{e}_n^{(\vec{B})}(x,x')\right|^2+\left|\vec{e}_n^{(\vec{B})}(y,y')\right|^2\right)^{\frac{1}{2}}. \tag{15}$$

Numerical integration of the magnitude of the 2-D noise electric field $\vec{e}_n\left((x,x'),(y,y')\right)$ over $x = 0$ to $x = W$ for all $y\in[0,W]$ and $y = 0$ to $y = W$ for all $x\in[0,D]$ provides the terminal voltages $v_t^{(\vec{B})}(x',y')$ due to the noise source at (x',y'), i.e.

$$v_t^{(\vec{B})}(x',y')=-\int_{x=0}^{x=D}\int_{y=0}^{y=W}\left|\vec{e}_n^{(\vec{B})}\left((x,x'),(y,y')\right)\right|dx\,dy. \tag{16}$$

The transfer impedance of the device at space point (x',y') is defined as

$$z_t^{(\vec{B})}(x',y')=\frac{v_t^{(\vec{B})}(x',y')}{i_n(x',y')}, \tag{17}$$

where $i_n(x',y')$ is the average current generated in the intervals dx' and dy' due to $\gamma(x')$ and $\gamma(y')$ located at x' and y' respectively. Now the mean-square noise voltage ($\langle v_{n(SC)}^2\rangle$) is obtained as [12]

$$\langle v_n^2\rangle^{(\vec{B})}=2q^2.df.A_j\int_{x=0}^{x=D}\int_{y=0}^{y=W}\left|z_t^{(\vec{B})}(x',y')\right|^2\left(\gamma(x')^2+\gamma(y')^2\right)^{\frac{1}{2}}dx'dy', \tag{18}$$

where A_j is the effective junction area of the device. Mean-square noise voltage per bandwidth is the noise spectral density (i.e. $\langle v_n^2\rangle^{(\vec{B})}/df$ V^2 s). The noise performance of the MAGTATT device in absence or presence of the magnetic field can be evaluated from a parameter known as the noise measure. This parameter is defined as [12], [28]

$$M_N^{(\vec{B})}=\frac{\langle v_n^2\rangle^{(\vec{B})}/df}{4k_BT\left(-Z_R^{(\vec{B})}(f)-R_S\right)}, \tag{19}$$

where $Z_R^{(\vec{B})}(f)$ is the negative resistance of the device which is a function of frequency and magnetic field [9], R_S is the positive parasitic series resistance of the device, k_B is the Boltzmann's constant (k_B = 1.38×10^{-23} J K^{-1}) and T is the absolute temperature in Kelvin (K).

V. Results and Discussion

The noise performance of the MAGTATT device under consideration has been investigated in this section in absence

of the magnetic field ($|B_z|$ = 0 T) as well as in present of the magnetic field ($|B_z|$ = 1.0 – 5.0 T) for the bias current densities of 2.6×10^8, 3.0×10^8, 3.4×10^8 and 3.8×10^8 A m^{-2}. Such high magnetic field can be practically produced by cryogenically-cooled superconducting electromagnet coil [29].

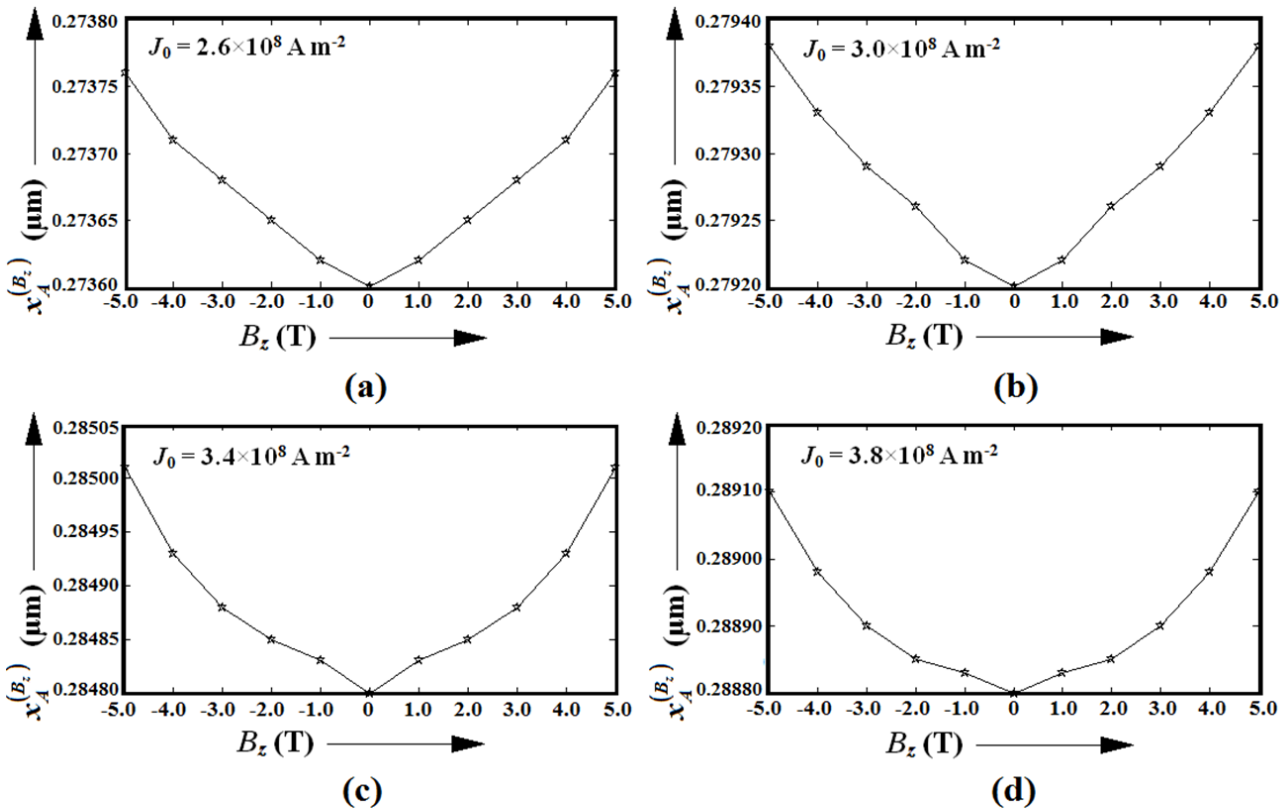

Fig. 2 Variations of avalanche zone width of MAGTATT device with applied transverse magnetic field for different bias current densities

The principal basis of noise in MAGTATT device is the random impact ionization phenomena within the avalanche zone of the device. Figs. 2 (a)-(d) show the variations of avalanche zone width of MAGTATT device with applied magnetic field varying from –5.0 to +5.0 T, for different bias current densities. It is observed from Figs. 2 (a)-(d) that the avalanche region of the device broadens due to the application of magnetic field. The width of the avalanche zone increases slightly with the increase of the magnitude of the transverse magnetic field. Deflection of charge carriers along $\pm x$ directions occurs depending on the polarities of those, due to the application of steady magnetic field along the perpendicular direction (along z-direction) to the direction of carrier movement (along y-direction). This, in turn, increases the effective depletion region width of the device for a given bias current density. Effective increment of the depletion region causes increase in the average kinetic energy of charge carriers moving under electric field by providing those extra regions for drift. This ensures premature growth of the impact ionization followed by charge multiplication phenomena. Therefore the total generation regions at both sides of the metallurgical junction widen in order to support the extra ionizing collisions. Sensitivity of the avalanche width with respect to the magnetic field (directed perpendicular to the carrier motion within the device) can be defined as [9]

$$S_X = \left|\frac{\Delta x_A^{(B_z)}}{\Delta B_z}\right|_{B_z=B_f}, \tag{20}$$

where $\Delta B_z = B_f - B_i$, B_f is the value of the magnetic field for which the sensitivity is to be calculated and B_i is the value of the magnetic field just earlier than B_f. The subscript of (20) indicates that the sensitivity is calculated for $B_z = B_f$. The magnetic field sensitivity of avalanche width of the MAGTATT device varies from 0.2×10^{-4} to 0.5×10^{-4} μm T^{-1} for the increase of magnetic field from 0.0 to ±5.0 T for the bias current density of 2.6×10^8 A m^{-2}. Thus broader avalanche region due to the presence of the transverse magnetic field indicates greater amount of random ionizing collisions with leads to increase the avalanche noise under reverse bias.

Fig. 3 shows the variations of noise spectral density ($\langle v_n^2\rangle^{(B_z)}/df$) of MAGTATT device with frequency for different applied transverse magnetic fields ($|B_z|$ = 0.0 – 5.0 T) for the bias current density of 2.6×10^8 A m^{-2}. It is interesting to observe from Fig. 3 that at lower frequencies, smaller than the optimum frequency of the device [9], noise spectral density decreases with the increase of the applied transverse magnetic

field. However, near the optimum frequency of the device, noise spectral density attains its peak value; and this peak noise spectral density of the device increases significantly with the increase of the applied transverse magnetic field. Under the practical operating conditions, the device mounted inside the cavity is tuned to the optimum frequency via mechanical and electronic tuning provisions in order to achieve highest RF power output. Therefore, under practical operating conditions, the noise spectral density of the device should attain the value near to its peak value. Thus peak noise spectral density determines the noise performance of the device. Figs. 4 (a) and (b) show the variations of peak noise spectral density of MAGTATT device with the frequency associated with that peak as well as with applied transverse magnetic field for different bias current densities. It is noteworthy from Figs. 4 (a) and (b) that for both the cases peak noise spectral density increases significantly with the increase of the bias current density.

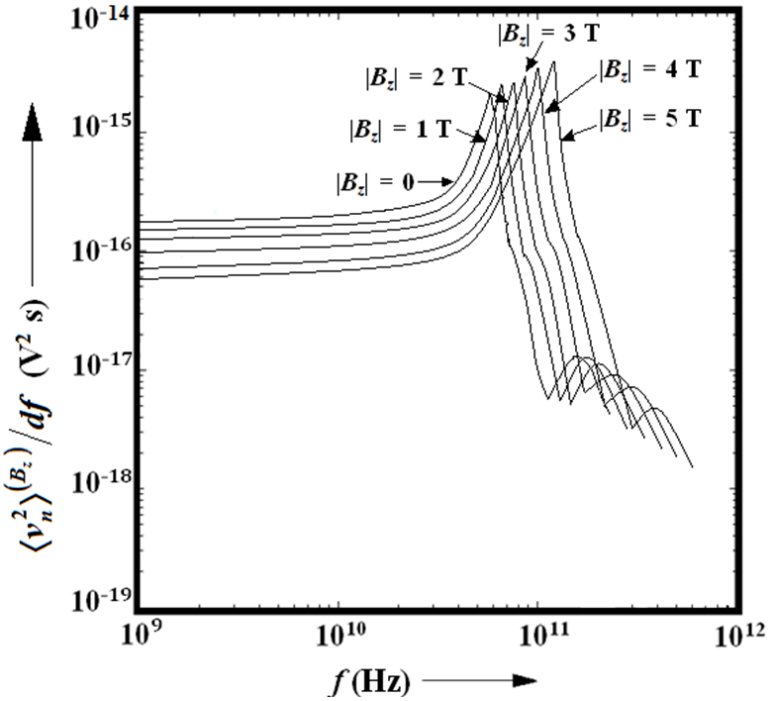

Fig. 3 Variations of noise spectral density of MAGTATT device with frequency for different applied transverse magnetic fields for the bias current density of 2.6×10^8 A m^{-2}

Variations of noise measure of MAGTATT device with frequency for different applied magnetic fields for the bias current density of 2.6×10^8 A m^{-2} have been shown in Fig. 5. The noise measure of the device as function of frequency has been calculated by assuming a fictitious value of the series resistance, i.e. $R_s = 0$ Ω. Later, the effect of series resistance on the noise measure of the device has been studied. It is observed that the noise measure of the MAGTATT device attains is minimum value at a frequency near to the optimum frequency of the device. This minimum value is corresponding to the peak value of the negative resistance ($Z_R^{(B_z)}(f)$) of the device at that frequency. Under practical operating conditions, this minimum value of the noise measure of the device is important because under these conditions, the device is tuned to the optimum frequency as mentioned earlier. It is observed from Fig. 5 that the minimum value of the noise measure increases with the increase of the magnitude of applied transverse magnetic field. Figs. 6 (a) and (b) show the variations of minimum noise measure of MAGTATT device with the frequency associated with that minimum as well as as with applied transverse magnetic field for different bias current densities for $R_s = 0$ Ω. Again, it is noteworthy that the minimum value of noise measure reduces significantly with the increase of the bias current density. The magnitude of the negative resistance of the device increases considerably with the increase of the bias current density [9]. This increment of the magnitude of the negative resistance dominates the enhancement in the noise spectral density due to the increase in bias current density by several orders. Therefore, the denominator of (19) dominates over the numerator of the same. Consequently, inverse relation of noise measure with the bias current density seizes.

Now the realistic values of series resistance have been taken into account while calculating the noise measure of the MAGTATT device under consideration designed to operate at W-band. The series resistance values ranging from 0-0.5 Ω have been considered for the present study. This range of values is quite realistic for W-band DDR IMPATTs [21].

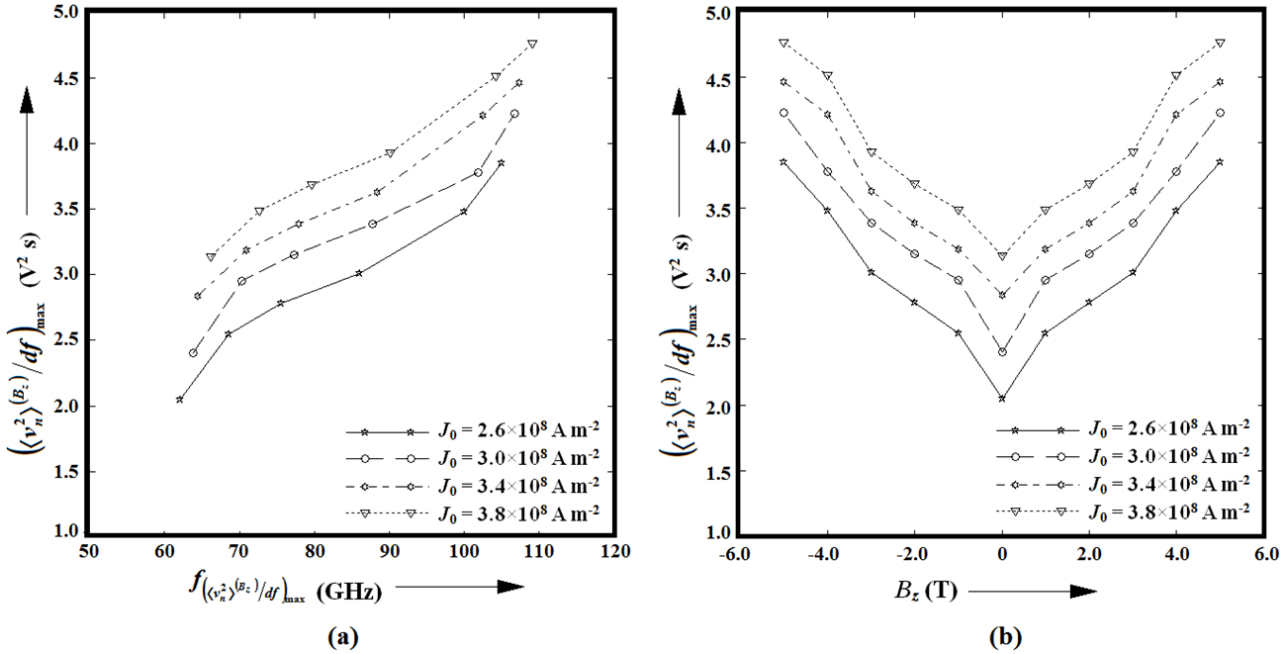

Fig. 4 Variations of peak noise spectral density of MAGTATT device with (a) the frequency associated with that peak and with (b) applied transverse magnetic field for different bias current densities

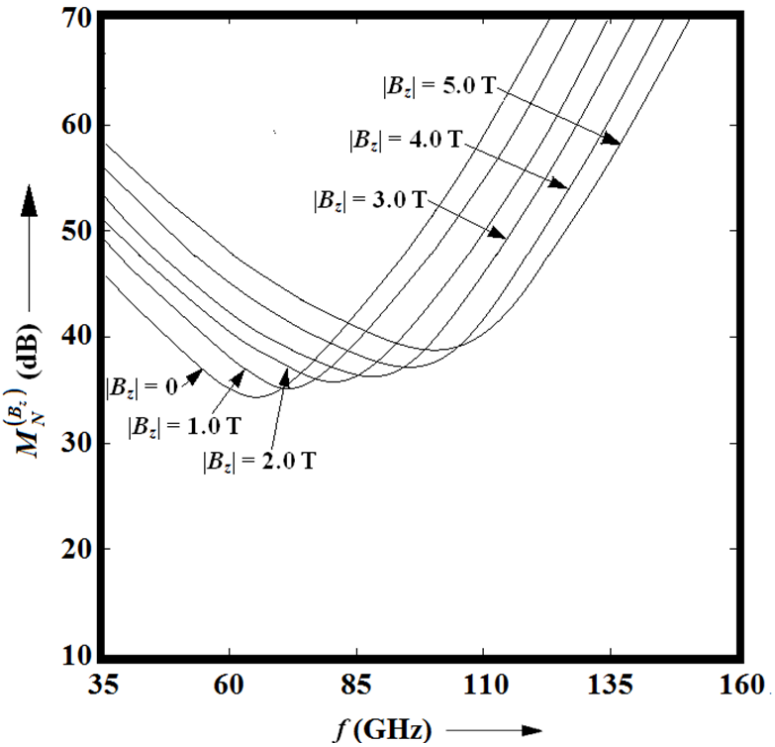

Fig. 5 Variations of noise measure of MAGTATT device with frequency for different applied transverse magnetic fields for the bias current density of 2.6×10^8 A m^{-2} (assuming $R_s = 0$ Ω)

Fig. 7 shows minimum noise measure of MAGTATT device with parasitic series resistance values for different applied transverse magnetic field at the bias current density of 2.6×10^8 A m^{-2}. It is observed from Fig. 7 that the noise measure increases significantly with the increase of the value of the series resistance. It is occurred since by increasing the value of R_s, the factor $\left(\left|Z_R^{(\bar{B})}(f)\right| - R_s\right)$ at the denominator of (19)

decreases, which leads to increase in noise measure. Therefore, it can be concluded that, to keep the noise measure minimum, the series resistance of the device has to be kept as small as possible by proper design and fabrication of the device [18], [30], [31]. This fact has to be followed in order to obtain maximum RF power output from the device [18], [30], [31]. The minimum noise measure along with maximum RF power output is achievable for $R_s = 0\ \Omega$.

The 1-D noise analysis of DDR Si IMPATT device designed to operate at W-band was reported by the authors earlier and noise measure of around 33-37 dB was obtained at the said frequency regime [16]-[19]. The 2-D noise simulation of the similar structure presented in this paper shows that the noise measure of it varies from 31.0 to 35.5 dB in absence of the magnetic field. The present 2-D simulation is expected to provide refined results as compared to the earlier one. However, the noise measure is observed to be increased significantly even above 38 dB in presence of the transverse magnetic field, which is an interesting and significant result. It was already reported that both the frequency and power tuning of the IMPATT devices are possible in considerable extent by means of transverse magnetic field [9] which can be considered as an additional terminal other than the bias current for tuning the power and frequency of IMPATT oscillators just like the optical tuning mechanism [17], [19]. But the results presented in this work indicate that the application of the magnetic field degrades the noise performance of the device. Analogous degradation of the noise performance of the device was observed earlier by the authors during the optical tuning of the IMPATT sources [16]-[19].

VI. Conclusion

The provisions for the frequency and power tuning of the MAGTATT devices by using the transverse magnetic field were already reported by the authors in their earlier work [9]. The current study deals with the development of 2-D model for investigating the noise performance of MAGTATT devices. A 2-D model has been developed by the authors to study the noise performance of MAGTATT device based on Si designed to operate at W-band. It is found that the application of the magnetic field degrades the noise performance of the device. The noise performance of the source has to be sacrificed in some extent for implementing the magnetic field tuning of the RF properties of IMPATT sources. Moreover, the knowledge of this effect clearly indicates that an IMPATT source must be covered with appropriate magnetic shielding material in order to avoid undesirable shift in operating frequency and output power as well as unintentional increase of avalanche noise due to the presence of external magnetic field.

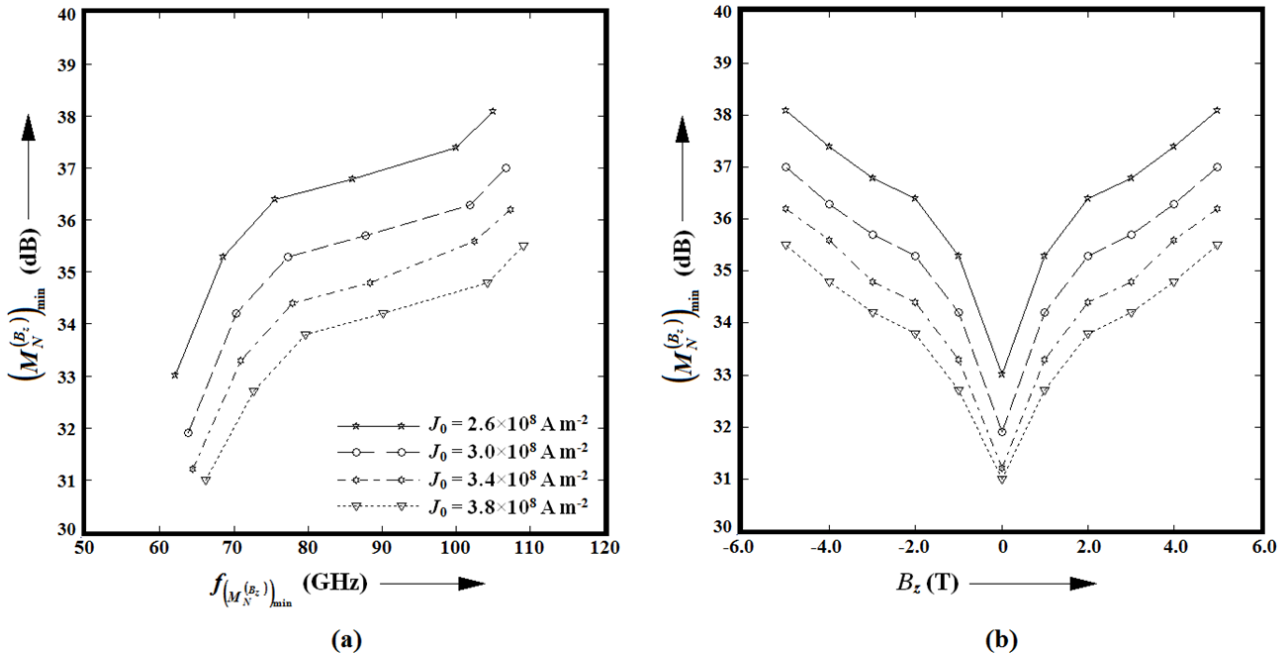

Fig. 6 Variations of minimum noise measure of MAGTATT device with (a) the frequency associated with that minimum and with (b) applied transverse magnetic field for different bias current densities (assuming $R_s = 0\ \Omega$)

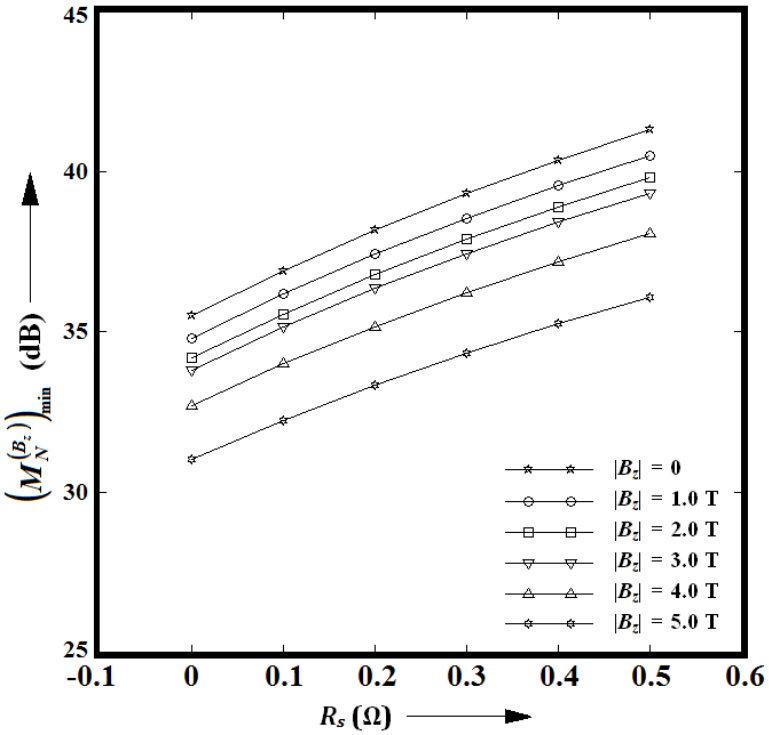

Fig. 7 Variations of minimum noise measure of MAGTATT device with series resistance for different applied transverse magnetic field at the bias current density of 2.6×10^8 A m^{-2}

ACKNOWLEDGMENT

Dr. Aritra Acharyya wishes to thank Cooch Behar Government Engineering College, WB, India, for providing excellent research facilities for carrying out the present work. Dr. Arindam Biswas wishes to thank Science and Engineering Research Board (SERB), India, for providing financial support for carrying out this research work through Early Career Research (ECR) Award scheme [grant number ECR/2017/000024/ES].

REFERENCES

[1] M. Gilden, and M. E. Hines, "Electronic tuning effects in Read microwave avalanche diode," *IEEE Trans. on Electron. Devices*, vol. 13, pp. 169-175, 1966.
[2] A. Schweighart, H. P. Vyas, J. M. Borrego, and R. J. Gutmann, "Avalanche diode structure suitable for microwave-optical interaction," *Solid-Sate Electron.* , vol. 21, pp. 1119-1121, 1978.
[3] H. P. Vyas, R. J. Gutmann, and J. M. Borrego, "Effect of hole versus electron photocurrent on microwave-optical interactions in impatt oscillators," *IEEE Transactions on Electron Devices*, vol. 26, pp. 232-234, 1979.
[4] J. R. Forrest, and A. J. Seeds, "Optical injection locking of impatt oscillators," *Electronics Letters*, vol. 14, pp. 626-627, 1978.
[5] A. J. Seeds, and A. Augusto, "Optical control of microwave semiconductor devices," *IEEE trans. on Microwave Theory and Techniques*, vol. 38, pp. 577-585, 1990.
[6] B. Glance, "A Magnetically Tunable Microstrip IMPATT Oscillator," *IEEE Transaction of Microwave Theory and Techniques*, vol. 21, pp. 425-426, 1973.
[7] R. A. Pucel, and D. J. Mass "Microstrip propagation on magnetic substrates—Part I: Design theory," *IEEE Trans. Microwave Theory Tech*., vol. 20, pp. 304-308, 1972.
[8] H. L. Hartnagel, G. P. Srivastava, P. C. Mathur, and V. Sharma, "Effect of Transverse Magnetic Field on the Power Output and Frequency of IMPATT Oscillators," *physica status solidi (a)*, vol. 3, pp. 1K147-K149, 1975.
[9] P. Banerjee, A. Acharyya, A. Biswas, and A. K. Bhattacharjee, "Effect of Magnetic Field on the RF Performance of Millimeter-Wave IMPATT Source," *Journal of Computational Electronics*, vol. 15, pp. 210-221, 2016.
[10] A. S. Tager, "Current fluctuations in semiconductor (dielectric) under the conditions of impact ionization and avalanche breakdown," *Sov. Phys. Solid State*, vol. 4, pp. 1919-1925, 1965.
[11] M. E. Hines, "Noise theory of Read type avalanche diode," *IEEE Trans. Electron Devices*, vol. 13, pp. 158-163, 1966.
[12] H. K. Gummel, and J. L. Blue, "A small-signal theory of avalanchenoisein IMPATT diodes," *IEEE Trans. on Electron Devices*, vol. 14, pp. 569-580, 1967.
[13] R. L. Kuvas, "Noise in IMPATT diodes: Intrinsic properties," *IEEE Trans. Electron Devices*, vol. 19, pp. 220-233, 1972.
[14] G. N. Dash, J. K. Mishra, and A. K. Panda, "Noise in Mixed Tunneling Avalanche Transit Time (MITATT) diodes," *Solid State Electronics*, vol. 39, pp. 1473-1479, 1996.
[15] J. K. Mishra, A. K. Panda, and G. N. Dash, "An extremely low-noise heterojunction IMPATT," *IEEE Trans. Electron Devices*, vol. 44, 2143-2148, 1997.
[16] A. Acharyya, M. Mukherjee, and J. P. Banerjee, "Noise Performance of Millimeter-wave Silicon Based Mixed Tunneling Avalanche Transit Time (MITATT) Diode," *International Journal of Electrical and Electronics Engineering*, vol. 4, 577-584, 2010.
[17] A. Acharyya, S.Banerjee, and J. P. Banerjee, "Effect of Photo-Irradiation on the Noise Properties of Double-Drift Silicon MITATT Device," *International Journal of Electronics*, vol. 101, pp. 1270-1286, 2014.
[18] P. Banerjee, Q. Hao, A. Biswas, A. K. Bhattacharjee and A. Acharyya, "Avalanche Noise in Magnetic Field Tunable Avalanche Transit Time Device," *in Proceedings of IEEE International Conference on Computer, Electrical and Communication Engineering (ICCECE), Kolkata, West Bengal, India*, 16th and 17th December, pp. 1-4, 2016, DOI: 10.1109/ICCECE.2016.8009570.
[19] A. Acharyya, "RF Performance of IMPATT Sources and Their Optical Control," *Lambert Academic Publishing, Germany*, 2015.
[20] A. Acharyya, S.Banerjee, and J. P. Banerjee, "Effect of Junction

Temperature on the Large-Signal Properties of a 94 GHz Silicon Based Double-Drift Region Impact Avalanche Transit Time Device," *Journal of Semiconductors*, vol. 34, pp. 024001-12, 2013.
[21] J. F. Luy, A. Casel, W. Behr, and E. Kasper, "A 90-GHz double-drift IMPATT diode made with Si MBE," *IEEE Trans. Electron Devices*, vol. 34, pp. 1084-1089, 1987.
[22] H. Pfleiderer, "Magnetodiode model," *Solid-State Electron.*, vol.15, pp. 335-353, 1972.
[23] A. Acharyya, J. Goswami, S.Banerjee, and J. P. Banerjee, "Estimation of Most Favorable Optical Window Position Subject to Achieve Finest Optical Control of Lateral DDR IMPATT Diode Designed to Operate at W-Band," *Radioengineering*, vol.23, pp. 739-753, 2014.
[24] H. P. Baltes, L. Andor, A. Nathan, and H. G. Schmidt-Weinmar, "Two-Dimensional Numerical Analysis of a Silicon Magnetic Field Sensor," *IEEE Transactions on Electron Devices*, vol. 31, pp. 996-999, 1984.
[25] M. Kurata, "Numerical Analysis for Semiconductor Devices," *Lexington MA*: *Heath*, 1982.
[26] H. H. Heimeier, "A two-dimensional numerical analysis of a silicon *n-p-n* transistor," *IEEE Trans. Electron Devices*, vol.20, pp. 708-714, 1973.
[27] M. Rudan, and R. Guerrieri, "Relevant problems in the numerical simulation of semiconductor devices using the finite element method," *in Numerical Analysis of Semiconductor Devices and Integrated Circuits, J. J. H. Miller, Ed. Dublin: Boole*, 1983.
[28] H. A. Haus, H. Statz, and R. A. Pucel, "Optimum noise measure of IMPATT diode," *IEEE Trans. on MTT*, vol. 19, pp. 801-813, 1971.
[29] T. Semba, T. Yamamoto, Y. Murata, M. Abe, S. Koda, Y. Iwasaki, Y. Takabayashi, and T. Kaneyasu, "Design and Manufacture of Superconducting Magnet for the Wiggler in Saga-LS," *Proceedings of IPAC'10, Kyoto, Japan*, pp. 358-360, 2010.
[30] A. Acharyya, S.Banerjee, and J. P. Banerjee, "Influence of Skin Effect on the Series Resistance of Millimeter-Wave of IMPATT Devices," *Journal Computational Electronics*, vol. 12, pp. 511-525, 2013.
[31] A. Acharyya, S.Banerjee, and J. P. Banerjee, "A Proposed Simulation Technique to Study the Series Resistance and Related Millimeter-Wave Properties of Ka-Band Si IMPATTs from the Electric Field Snap-Shots," *International Journal of Microwave and Wireless Technologies*, vol. 5, 91-100, 2013.
[32] T. A. Midford, and R. L. Bernick, "Millimeter Wave CW IMPATT diodes and Oscillators," *IEEE Trans. Microwave Theory Tech*., vol. 27, pp. 483-492, 1979.

Partha Banerjee is presently carrying out his doctoral research at National Institute of Technology, Dugapur, WB, India. His research interests are high frequency semiconductor devices.

Dr. Aritra Acharyya was born in 1986. He received B.E. and M.Tech. degrees from IIEST, Shibpur, India, and Institute of Radio Physics and Electronics, University of Calcutta, India, in the years 2007 and 2010 respectively. Finally he obtained Ph.D. degree from Institute of Radio Physics and Electronics, University of Calcutta, in the year 2016. He is currently working as an Assistant Professor of Electronics and Communication Engineering Department at Cooch Behar Government Engineering College, West Bengal. His research interests are high frequency semiconductor devices. He has already published more than 115 research papers in peer reviewed journals and conference proceedings.

Dr. Arindam Biswasreceived B.Tech. and M.Tech. degrees from Dumkal Institute of Engineering and Technology, WB, India, and Institute of Radio Physics and Electronics, University of Calcutta, in the years 2007 and 2010 respectively. Finally he obtained Ph.D. degree from National Institute of Technology, Dugapur, WB, India, in the year 2013. His research interests are non-linear optics and high frequency semiconductor devices.

Dr. A. K. Bhattacharjee is currently working as a Professor of ECE Department in National Institute of Technology, Dugapur, WB, India. His research interests are antenna and high frequency semiconductor devices.